


# Does chemical shift imaging offer a biomarker for the diagnosis and assessment of disease severity in multiple myeloma?

## A cross-sectional study

Miyuki Takasu, MD<sup>a,\*</sup> , Keizo Tanitame, MD<sup>b</sup>, Yasutaka Baba, MD<sup>a</sup>, Yuji Akiyama, RT<sup>a</sup>, Takayuki Tamura, RT<sup>a</sup>, Shota Kondo, MD<sup>a</sup>, Shogo Maeda, MD<sup>a</sup>, Akira Sakai, PhD<sup>c</sup>, Kazuo Awai, PhD<sup>a</sup>

### Abstract

To investigate whether chemical shift imaging (CSI) is useful for differentiating myelomatous infiltration from hematopoietic bone marrow (BM) and for quantitatively assessing disease severity.

In this retrospective study, spinal MRI, including a sagittal iterative decomposition of water and fat with echo asymmetry and least-squares estimation T2 fast spin-echo sequence, was performed on 76 myeloma patients (45 men, 67.0±11.4 years; 31 women, 66.5±11.0 years) and 30 control subjects (20 men, 67.0±8.4 years; 10 women, 67.0±9.2 years). The fat-signal fraction (FF) and mean signal dropout ratio (DR) were calculated from lumbar BM that contained no focal lesions. The BM plasma cell percentage (BMPC%) and serological data were obtained. As DR is highest when FF=50%, the patients were divided into 2 groups: a water-dominant group (FF<50%) and a fat-dominant group (FF > 50%).

Serum monoclonal protein (M protein), β2-microglobulin, and BMPC% were significantly higher in the water-dominant group than in the fat-dominant group. In the water-dominant group, DR correlated significantly with BMPC% and M protein, whereas in the control group, DR showed a weak correlation with age but no correlation with other clinical factors. No significant differences in any clinical data were seen between high and low DR.

CSI proved ineffective for differentiating myelomatous infiltration from hematopoietic BM. For myeloma patients with relatively high BM cellularity, a small signal drop on opposed-phase images indicated a higher tumor burden. For BM with relatively low cellularity, disease severity was not reflected by CSI.

**Abbreviations:** ADC = apparent diffusion coefficient, BM = bone marrow, BMPC% = BM plasma cell percentage, CSI = chemical shift imaging, DR = dropout ratio, FF = fat-signal fraction, FSE = fast spin echo, IDEAL = iterative decomposition of water and fat with echo asymmetry and least-squares estimation, IP = in-phase, M protein = monoclonal protein, MM = multiple myeloma, MRI = magnetic resonance imaging, OP = opposed-phase, ROIs = regions of interest.

**Keywords:** chemical shift imaging, MRI, multiple myeloma

## 1. Introduction

Multiple myeloma (MM) is a hematological malignancy characterized by the clonal expansion of plasma cells within the bone marrow (BM). The pattern of BM infiltration on magnetic resonance imaging (MRI) has been reported to have

prognostic significance in newly diagnosed patients with symptomatic disease.<sup>[1–3]</sup> For example, Mouloupoulos et al<sup>[1]</sup> reported that the median overall survival of patients with newly diagnosed MM was significantly shorter if they had a diffuse MRI pattern compared with variegated and normal patterns. In patients with smoldering MM, diffuse marrow infiltration on

Editor: Alauldeen Mudhafar Zubair Alqasim.

This work was supported by Grants-in-aid for Scientific Research (JSPS KAKENHI No. 17K10406, to M.T.) from the Japanese Ministry of Education, Culture, Sports, Science, and Technology; and by a Research Grant from the International Myeloma Foundation Japan, 2012.

M.T.: Kyowa Kirin Co., Ltd., Celgene Co.; K.A.: Research grants from Canon Medical Systems Corporation, Hitachi Ltd., Fujitsu Ltd., Eisai Co., Ltd., Nemoto Kyorindo Co., Ltd., and Fuji Pharma Co., Ltd. Remaining authors have no conflicts of interest to disclose.

All data generated or analyzed during this study are included in this published article [and its supplementary information files].

<sup>a</sup> Department of Diagnostic Radiology, Graduate School of Biomedical Sciences, Hiroshima University, <sup>b</sup> Department of Radiology, Hiroshima Prefectural Hospital, Hiroshima, <sup>c</sup> Department of Radiation Life Sciences, Fukushima Medical University School of Medicine, Fukushima, Japan.

\* Correspondence: Miyuki Takasu, 1-2-3 Kasumi, Minami-ku, Hiroshima-shi, 734-8551, Japan (e-mail: my-takasu@syd.odn.ne.jp).

Copyright © 2021 the Author(s). Published by Wolters Kluwer Health, Inc.

This is an open access article distributed under the terms of the Creative Commons Attribution-Non Commercial License 4.0 (CCBY-NC), where it is permissible to download, share, remix, transform, and buildup the work provided it is properly cited. The work cannot be used commercially without permission from the journal.

How to cite this article: Takasu M, Tanitame K, Baba Y, Akiyama Y, Tamura T, Kondo S, Maeda S, Sakai A, Awai K. Does chemical shift imaging offer a biomarker for the diagnosis and assessment of disease severity in multiple myeloma? A cross-sectional study. *Medicine* 2021;100:6(e24358).

Received: 25 November 2019 / Received in final form: 21 October 2020 / Accepted: 22 December 2020

<http://dx.doi.org/10.1097/MD.00000000000024358>

MRI was also associated with increased risk for progression.<sup>[4]</sup> Although an infiltration pattern on MRI has been demonstrated as a reliable biomarker for predicting prognosis,<sup>[1,2]</sup> it has not been included in any criteria for MM because the assessment of nonfocal tumor infiltration on MRI can be subjective. In addition, variegated or diffuse patterns may be normal variations or indicate a physiological process such as hematopoietic BM. There is therefore a need for an objective MRI biomarker for quantifying tumor mass and for increasing the specificity of abnormal signal in BM.

Chemical shift imaging (CSI) was originally described in 1984 as a 2-point Dixon method that can provide both in-phase (IP) and opposed-phase (OP) images,<sup>[5]</sup> and is based on the principle that protons attached to water and to fat precess at different frequencies. Signal intensity is derived from the sum of signals from fat and water spins on IP images and from the difference between those signals on OP images. For example, in a voxel representing an area containing fat and water, which is common in hematopoietic BM, there is an additive effect on the signal in the IP image and a loss of signal of at least 20% in the OP image.<sup>[6,7]</sup> If the voxel represents tumor that has replaced normal fatty marrow, the voxel represents only water and there is no significant drop in signal on the OP image compared with the IP image. It is important to emphasize that CSI does not differentiate between benign and malignant lesions, but rather between BM-replacing and non-BM-replacing lesions. Because hematopoietic BM and infiltrative MM can demonstrate a similar degree of signal drop on OP images, hematopoietic BM can provide a false-positive diagnosis of infiltrative MM on OP imaging due to the presence of both fat and water cells, as reported previously.<sup>[8]</sup>

Advances in MRI technology have led to the development of 3-point Dixon techniques. Iterative decomposition of water and fat with echo asymmetry and least-squares estimation (IDEAL) MRI can provide four sets of image types in a single session using the chemical-shift effect: water-only, IP, OP, and fat-only images.<sup>[9]</sup> In addition, the IDEAL technique can provide a quantitative measure of fat content and degree of signal drop for liver and BM on OP images.<sup>[10–14]</sup>

The purpose of this study was to investigate whether signal dropout ratio (DR) in lumbar BM calculated from CSI is useful for differentiating myelomatous infiltration from hematopoietic BM and for quantitative assessment of disease severity.

## 2. Materials and methods

### 2.1. Ethics Statement

This retrospective, single-institution study was approved by the Institutional Review Board of Hiroshima University Hospital, with a waiver of informed consent. Patient records and information were anonymized and de-identified before analysis.

### 2.2. Subjects

We searched the computerized database and reviewed the medical records of all patients who had been seen at Hiroshima University Hospital between May 2010 and April 2014, before the upgrade of the MRI unit after 2014. The diagnostic criteria were taken from the those established by the International Myeloma Working Group.<sup>[15]</sup> After excluding patients who had undergone chemo- or radiotherapy, the remaining 45 men (mean age,  $67.0 \pm 11.4$  years; range, 41–89 years) and 31 women (mean age,  $66.5 \pm 11.0$  years; range, 46–84 years) with newly diagnosed MM were included in the study and statistical analyses. Of these 76 myeloma patients, 9 had smoldering myeloma and 67 had symptomatic myeloma. No serial examinations were included.

Subjects in an age-matched control group (20 men (mean age,  $67.0 \pm 8.4$  years; range, 41–87 years); 10 women ( $67.0 \pm 9.2$  years; range, 46–80 years)) were selected randomly from our hospital's radiology information system. The controls had undergone MRI of the lumbar spine to rule out metastatic spinal tumors in the investigation of back or leg pain, using the same scanning protocol as the myeloma patients.

All subjects were Japanese.

### 2.3. Spinal MRI and quantitative study

Imaging was performed using a 3.0-T MRI unit (Signa HDxt, GE Healthcare, Milwaukee, WI) and the following sequences (Table 1): sagittal T1 fast spin echo (FSE), sagittal FS-T2 FSE (with chemical shift selective technique), and sagittal IDEAL T2 FSE sequence. The MRI scanner underwent routine calibration scans and phantom assessments to monitor image quality and signal-to-noise ratio. All sequences, including IDEAL, are commercially available (GE Healthcare). Co-registered water, fat, IP, and OP images were generated using commercially available IDEAL software on the operator console. A detailed description of the IDEAL FSE sequence has been published by Reeder et al.<sup>[9]</sup> Using a product version of IDEAL, we acquired 3 images at optimized phase angles of  $-\pi/6$ ,  $\pi/2$ , and  $7\pi/6$ .<sup>[9]</sup> To avoid water/fat swaps, a region-growing algorithm was employed for field-map estimation.

Mean signal intensity and standard deviation were calculated by placing operator-determined regions of interest (ROIs) within BM that contained no focal lesions. ROIs were placed by a radiologist (M.T.) with 22 years of experience in spinal imaging, and defined manually within the internal parts of the L1-L3 vertebral bodies. These levels were chosen because they are less likely than lower lumbar elements to be affected by degenerative disc disease, and less likely than lower thoracic elements to be fractured (Fig. 1). The area of BM ROIs was 250 to 486 mm<sup>2</sup>. Signal intensity values were then calculated as the mean value obtained from these three vertebral bodies, as described

**Table 1**  
Acquisition parameters for MRI sequences.

Sequence	TR/TE/TI (ms)	NSA	FOV (mm)	Matrix	Slice thickness (mm)	Bandwidth (kHz)	Imaging time (min: s)
IDEAL T2 FSE	4000/112.4	3	300	384 × 192	4	83.3	5:12
Fat-suppressed T2 FSE	4000/116	2	300	320 × 288	4	62.5	2:16
T1 FSE	700/11.8	2	300	512 × 224	4	41.7	2:38

FOV = field of view, FSE = fast spine echo, IDEAL = iterative decomposition of water and fat with echo asymmetry and least-squares estimation, NSA = number of signal averages, TE = echo time, TI = inversion time, TR = repetition time.

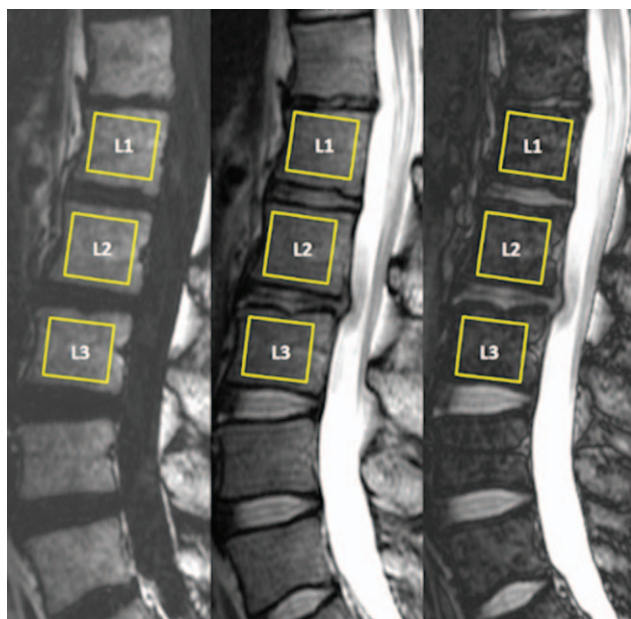


**Figure 1.** Calculation of fat-signal fraction and dropout ratio on a mid-sagittal MRI of the lumbar spine. A manually defined volume of interest is placed in the vertebral body of each of L1-L3, avoiding the cortex and endplates. Calculated fat (left), in-phase (middle), and opposed-phase (right) images are shown.

previously<sup>[12]</sup>. If one of the L1-L3 vertebrae was fractured or contained a focal osteolytic lesion with a long axis >0.5 cm, that vertebra was excluded from the calculation of fat-signal fraction (FF). All focal myelomatous lesions were confirmed as lytic

lesions by whole-body CT. Five patients were excluded from the study because 2 of the L1-L3 vertebrae were fractured or contained a focal osteolytic lesion, resulting in a total of 71 patients (42 men, 67.0±12.2 years; 29 women, 66.5±10.5 years).

The FF from the IDEAL images was calculated as the ratio of the signal intensity in the fat image divided by the signal intensity of the corresponding ROI in the IP image. Mean signal DR in the L1-L3 vertebral bodies was calculated as the ratio of the difference of signal-to-noise ratio between the IP and OP images to the signal-to-noise ratio of the IP image.

To evaluate small areas of possible myelomatous infiltration that had a central area of hyperintensity without the appearance of obvious focal lesion, we performed qualitative assessment of ring-like chemical shift artifact (ie, etching artifact) at the fat-water interface. Two of the authors (M.T., with 22 years of experience in spinal imaging; and K.T., with 20 years of experience in musculoskeletal imaging) reviewed the sagittal IP and OP images of each subject for the presence of etching artifact (Fig. 2) to analyze interobserver agreement and to assess the contribution of etching artifact to the diagnosis of small myelomatous infiltration. In the case of disagreement, agreement was reached by consensus, with adjudication by a board-certified radiologist (Y.B., with 22 years of experience).

**2.4. Bone marrow examination and serological data**

We estimated the proportion of BM plasma cells (BM plasma cell percentage [BMPC%]) in BM biopsy specimens obtained from the iliac crest of all patients. The mean interval between biopsy and MRI was 8 days (range, 3–14 days).

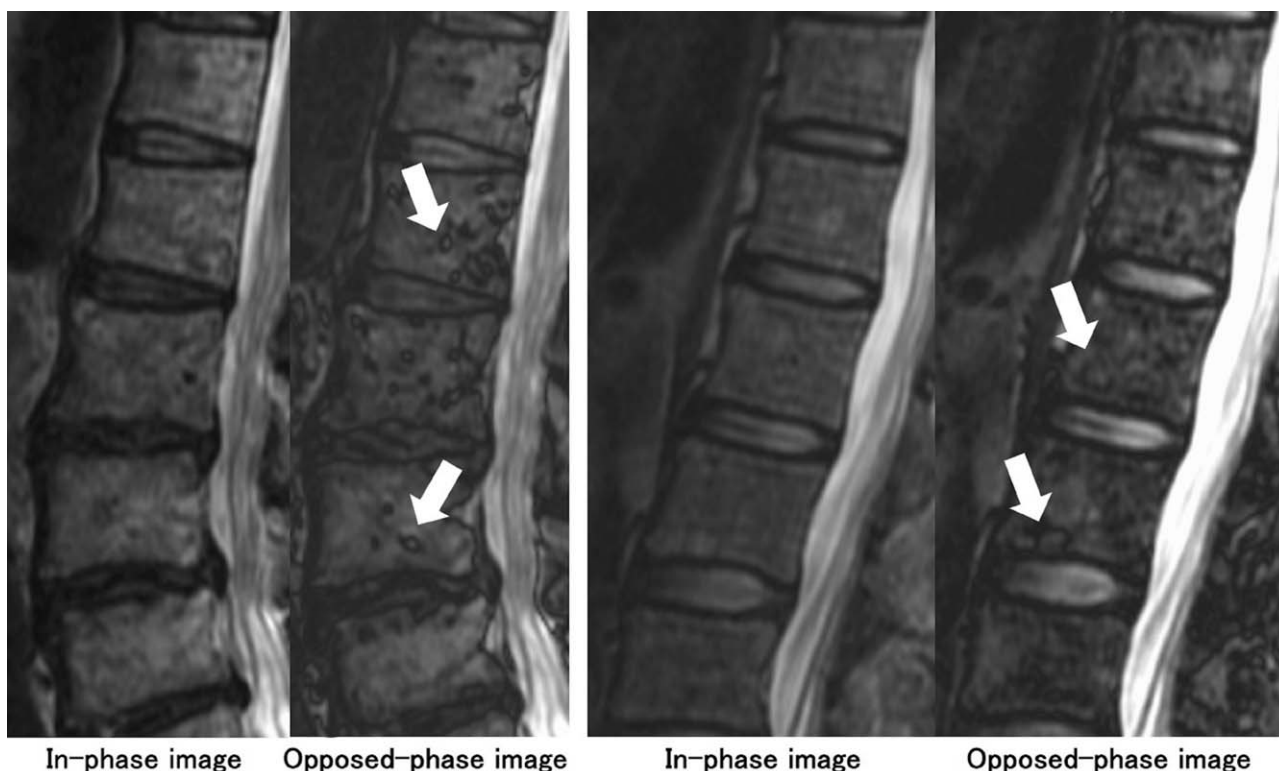


**Figure 2.** Ring-like chemical shift artifact (etching artifact, white arrows) is shown on sagittal opposed-phase images (white arrows). Left: a 65-year-old female control. Right: a 52-year-old woman with symptomatic myeloma.



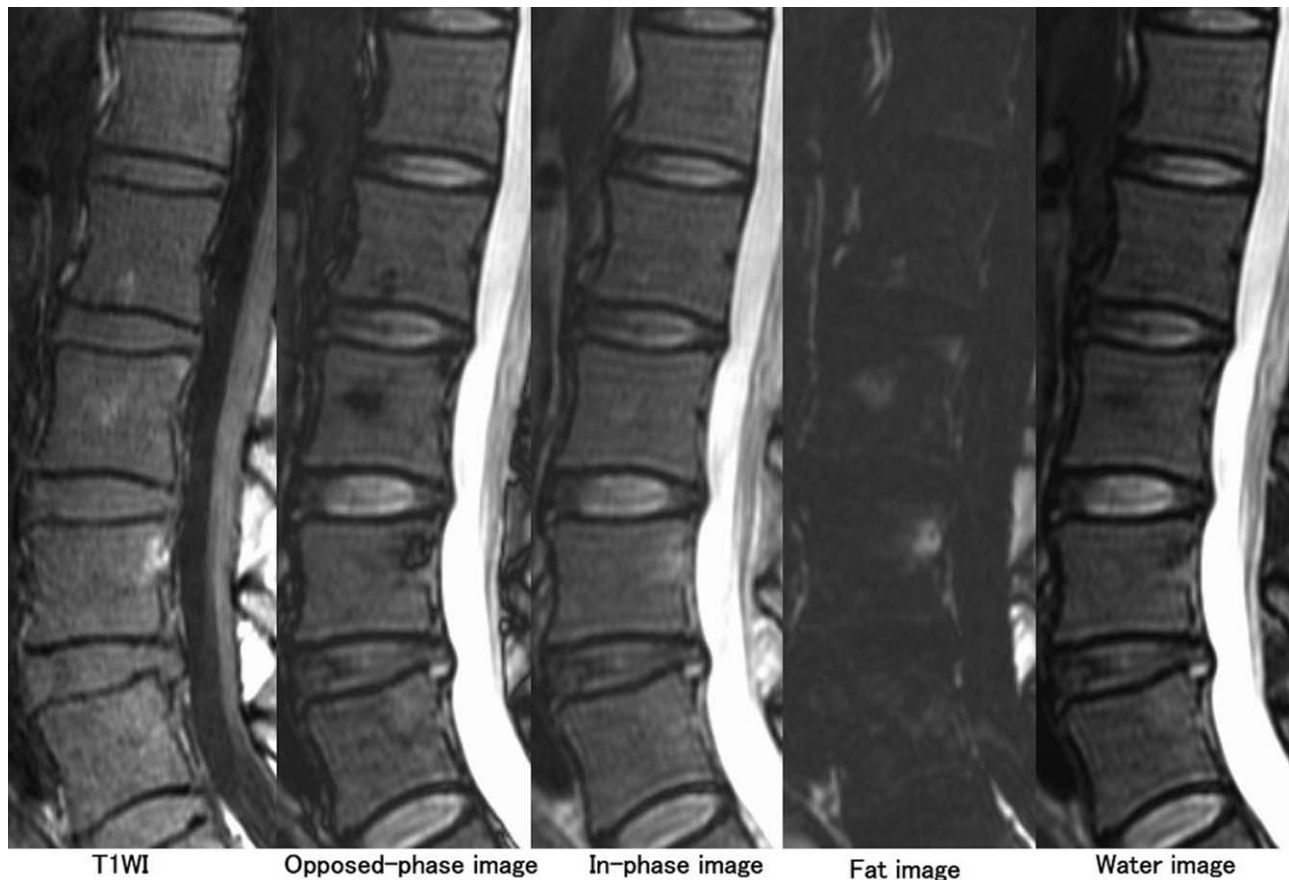


**Figure 3.** Sagittal MRI of a 46-year-old woman with symptomatic myeloma (water-dominant group: fat-signal fraction = 17.3%, dropout ratio = 36.0%). Serum monoclonal protein level was 9719 mg/dL,  $\beta_2$ -microglobulin was 3.41 mg/L, and bone marrow plasma cell percentage from the iliac crest was 50.0%. (A) T1-weighted image shows diffusely decreased signal intensity in the bone marrow. Bone marrow signal intensity in the opposed-phase image (B) is almost equal to that in the in-phase image (C), concordant with low dropout ratio. (D) Fat image. (E) Water image.

Serological data, including serum monoclonal protein (M protein), albumin,  $\beta_2$ -microglobulin,  $\kappa/\lambda$  ratio, and blood counts, were obtained in the myeloma patients and blood counts were obtained in the control subjects.

### 2.5. Statistical analysis

In data analysis, we divided the patients into 2 groups according to the amount of fat signal in the lumbar BM: water-dominant group (FF < 50%, n = 22, Fig. 3) and fat-dominant group (FF > 50%, n = 49, Fig. 4). We used a cutoff value of 50% because signal cancellation between fat and water protons and DR is highest when FF = 50%. Patients' characteristics, MRI-derived parameters, and serological data were compared among the water-dominant, fat-dominant, and control groups using one-way analysis of variance for normally distributed measures and the Kruskal-Wallis test for non-normally distributed measures, followed by the Steel-Dwass test. The Kolmogorov-Smirnov test was used to determine whether values were normally distributed. The Mann-Whitney *U* test was used to determine difference between the water- and fat-dominant groups. The chi-square test was used to test relationships between categorical variables. We calculated the Spearman correlation coefficients between DR and clinical parameters including BMPC%, serum M protein, albumin,  $\beta_2$ -microglobulin, hemoglobin, platelets, and white

blood cells for each patient group; and hemoglobin, platelets, and white blood cells for the control group. To explore the significance of degree in signal drop on the OP images in evaluating the disease severity of MM, we compared clinical parameters between patients with high DR (> 60%) and low DR (< 60%). This 60% cutoff value was chosen so that the number of patients was similar between the 2 groups. Values of  $P < .05$  were considered significant.

The Cohen kappa was used to measure inter-reader reliability for the presence or absence of etching artifact, for the reason that interpretation of such a small area can be subjective. Kappa values of 0.61 to 0.80 were considered to represent substantial agreement and those > 0.80 were considered to represent excellent agreement. The  $\chi^2$  test was used to analyze the difference in frequency of etching artifact between myeloma patients and controls.

All analyses were performed using a spreadsheet application (Excel 2019 version 3.2; Microsoft, Redmond, WA).

### 3. Results

Table 2 summarizes the patient characteristics and laboratory, MRI, and BM findings for the water-dominant group, fat-dominant group, and control subjects. There was no significant difference among the groups in terms of patient age or DR. In the

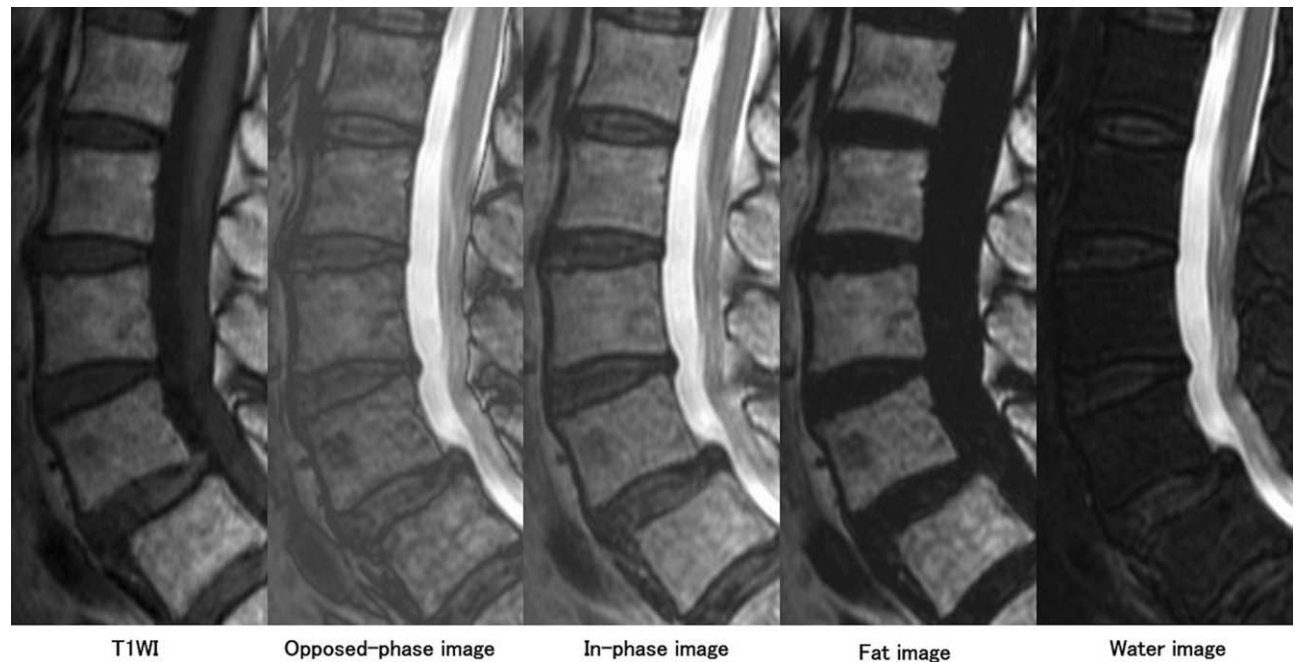


**Figure 4.** Sagittal MRI of a 58-year-old woman with symptomatic myeloma (fat-dominant group: fat-signal fraction = 80.8%, dropout ratio = 38.7%). Serum monoclonal protein level was 4980 mg/dL,  $\beta$ 2-microglobulin was 3.09 mg/L, and bone marrow plasma cell percentage from the iliac crest was 15.5%. (A) Signal intensity in the bone marrow is grossly homogeneous and higher than that of intervertebral discs on T1-weighted imaging. Bone marrow signal intensity in the opposed-phase image (B) is almost equal to that of the in-phase image (C), concordant with low dropout ratio. (D) Fat image. (E) Water image.

water-dominant group, serum M protein,  $\beta$ 2-microglobulin, and BMPC% were significantly higher and albumin was significantly lower than those in the fat-dominant group ( $P=.04$ ,  $P=.03$ ,  $P=.01$ ,  $P=.002$ , respectively). Abnormal serum free light chain ratio was detected significantly more frequently in the water-

dominant group than in the fat-dominant group ( $P<.0001$ ). Similar types of immunoglobulins (immunoglobulin G vs immunoglobulin A) were seen in the 2 patient groups.

In the water-dominant group, DR correlated significantly with BMPC% ( $\rho=-0.662$ ,  $P=.003$ ) and serum M protein ( $\rho=-0.586$ ,

**Table 2**

**Characteristics, laboratory, MRI, and bone marrow findings of the study population.**

	Water-dominant group	Fat-dominant group	Control subjects	P value
Sex				
Male (number of patients)	11	31	13	
Female (number of patients)	11	18	17	.47
Age (yrs)	67.3 $\pm$ 12.2	67.4 $\pm$ 11.2	61.0 $\pm$ 11.0	.46
Laboratory data				
Serum M protein			N/A	
M protein (mg/dl)	3966 $\pm$ 624	2717 $\pm$ 274		.04
IgG (number of patients)	19	44		
IgA (number of patients)	3	5		.67
Albumin (g/dl)	3.29 $\pm$ 0.20	4.04 $\pm$ 0.12		.002
$\beta$ 2-microglobulin (mg/l)	7.13 $\pm$ 1.77	3.27 $\pm$ 0.33	N/A	.01
Kappa/lambda ratio			N/A	
0.125–8 (number of patients)	8	46		
$\leq$ 0.125 or $\geq$ 8 (number of patients)	14	3		<.0001
Hemoglobin (g/dl)	11.5 $\pm$ 0.3*	9.4 $\pm$ 0.5†	15.0 $\pm$ 0.5	<.0001
Platelets ( $10^3/\mu$ l)	155 $\pm$ 18	189 $\pm$ 10	202 $\pm$ 21	.17
White blood cells ( $10^3/\mu$ l)	5.34 $\pm$ 0.30	5.15 $\pm$ 0.57	5.20 $\pm$ 0.35	.89
MRI data				
Dropout ratio	60.4 $\pm$ 1.96	60.6 $\pm$ 4.9	57.0 $\pm$ 2.4	.42
Bone marrow biopsy			N/A	
BMPC%	37.7 $\pm$ 6.9	17.2 $\pm$ 2.7		.01

\* Difference between water-dominant group and control subjects.

† Difference between fat-dominant group and control subjects.

BMPC%=bone marrow plasma cell percentage; N/A=not applicable.

**Table 3**  
Correlation between dropout ratio and clinical factors.

Variable	Water-dominant group		Fat-dominant group		Control subjects	
	$\rho$	<i>P</i>	$\rho$	<i>P</i>	$\rho$	<i>P</i>
Age (yrs)	0.264	.275	-0.263	.07	-0.409	.03*
Laboratory data						
Serum M protein (mg/dl)	-0.586	.008*	-0.047	.76	N/A	
Albumin (g/dl)	0.384	.11	0.093	.54	N/A	
$\beta$ 2-microglobulin (mg/l)	-0.270	.26	0.117	.45	N/A	
Hemoglobin (g/dl)	0.336	.16	0.161	.29	-0.137	.67
Platelets ( $10^3/\mu$ l)	-0.048	.85	-0.089	.59	-0.181	.57
White blood cells ( $10^3/\mu$ l)	-0.423	.07	0.077	.61	-0.573	.05
Bone marrow biopsy					N/A	
BMPC%	-0.662	.003*	0.069	.67		

$\rho$ , the Spearman correlation coefficient.

\* Indicates significant correlation ( $P < .05$ ).

BMPC% = bone marrow plasma cell percentage; N/A = not applicable.

$P = .008$ ; Table 3, Fig. 5). In the fat-dominant group, no significant correlation was found between DR and clinical factors. In the control group, DR showed a weak correlation with age ( $\rho = -0.409$ ,  $P = .03$ ) but no correlation with other clinical factors.

No significant differences in any clinical data were seen between high and low DR (Table 4, Fig. 6).

Interobserver agreement for evaluating the presence of etching artifact was substantial ( $\kappa = 0.71$ ). After reaching consensus, etching artifact was present in 21.1% of myeloma patients (15/71) and in 7.0% (2/30) of controls. There was no statistical difference in the frequency of etching artifact between myeloma patients and controls ( $P = .302$ ).

#### 4. Discussion

Normal hematopoietic marrow in the axial skeleton contains fat and water components. Red marrow has a fat content of

approximately 40% and yellow marrow has a fat content of approximately 80%.<sup>[6]</sup> Marrow infiltrative processes such as malignant neoplasms tend to replace the fatty marrow components completely. Therefore, CSI with IP and OP images has been described as a useful technique for evaluating BM, and especially for distinguishing marrow-replacing lesions from non-marrow-replacing processes. Zajick et al proposed a cut-off decrease of >20% of the signal intensity in OP imaging using in-phase and out-of-phase fast multiplanar spoiled gradient-echo MR imaging to predict malignancy in a vertebral body abnormality.<sup>[6]</sup> However, their analyses focused on internal parts of focal vertebral marrow abnormalities such as endplate degeneration or metastatic bone tumors, and did not include diffusely infiltrating tumor. Known potential pitfalls of OP imaging of BM include infiltrative MM, but the capability of OP imaging to differentiate between hematopoietic BM and myelomatous infiltration has not been fully investigated.

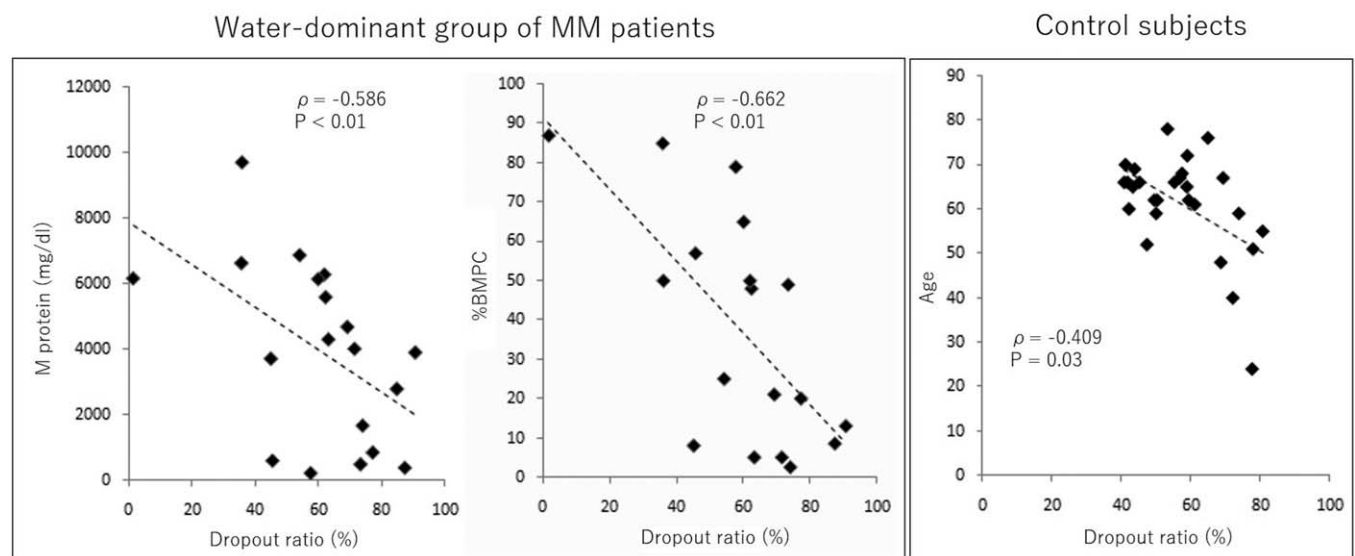


**Figure 5.** Spearman correlation coefficients between the DR of chemical shift imaging signal and clinical factors for patients with multiple myeloma. In the water-dominant group of myeloma patients, DR correlates significantly with serum monoclonal protein (M protein, left) and bone marrow plasma cell percentage (BMPC%, middle). In the control group, DR shows a weak correlation with age (right). DR = dropout ratio.

**Table 4****Comparison of clinical and laboratory data between high and low dropout ratio (DR) in patients with myeloma.**

Variable	High DR (> 60%)	Low DR (< 60%)	P value
Sex			
Male	19	23	
Female	13	16	.97
Age (yrs)	65.5±13.4	68.0±10.7	.44
Laboratory data			
Serum M protein (mg/dl)			
M protein	2830±373	3504±382	.38
IgG	30	33	
IgA	2	6	.82
Albumin (g/dl)	3.83±0.14	3.81±0.18	.94
β2-microglobulin (mg/l)	4.33±0.68	4.52±0.99	.87
Kappa/lambda ratio			
0.125-8	14	16	
≤0.125 or ≥8	18	23	.82
Hemoglobin (g/dl)	11.1±0.5	10.8±0.4	.58
Platelets (10 <sup>3</sup> /μl)	162±13	193±11	.09
White blood cells (10 <sup>3</sup> /μl)	5.04±0.35	5.49±0.41	.40
Bone marrow biopsy			
BMPC%	21.5±4.3	24.8±4.3	.58

BMPC%=bone marrow plasma cell percentage; DR=dropout ratio.

Evaluation of disease within BM by MRI is useful for monitoring the effects of chemotherapy, particularly as it is often necessary to discontinue treatment due to high treatment-related

toxicity.<sup>[17,18]</sup> In addition, it can be difficult to detect relapse after treatment because of the highly variable duration of disease control after therapy.<sup>[19]</sup> In these settings, the differentiation of myeloma relapse from the regrowth of hematopoietic BM plays a key role in determining the treatment strategy. To the best of our knowledge, the present report is the first to demonstrate that CSI is not useful for differentiating myelomatous infiltration from hematopoietic BM.

We found no significant difference in DR between myeloma patients and controls, in agreement with the findings of a previous report<sup>[20]</sup> that showed the potential pitfalls of using CSI for patients with hematopoietic BM (including infiltrative myeloma), given that signal dropout on the OP image is due to the presence of both fat and water protons in the same voxel for both conditions. We also found no significant difference in the frequency of etching artifact between myeloma patients and controls. We consider that normal isolated hematopoietic foci and small possible myelomatous focal lesions do not demonstrate a signal drop on OP images because there is no signal cancellation between fat and water protons in these areas. In the present study, DR did not differ significantly between the fat-dominant and water-dominant groups. This finding might be explained similarly: that little signal cancellation occurs between fat and water spins in the fat-dominant and water-dominant BM components.

Another MRI sequence used for evaluating BM for MM is diffusion-weighted imaging with calculation of apparent diffusion coefficient (ADC). Koutoulidis et al<sup>[21]</sup> established a cutoff

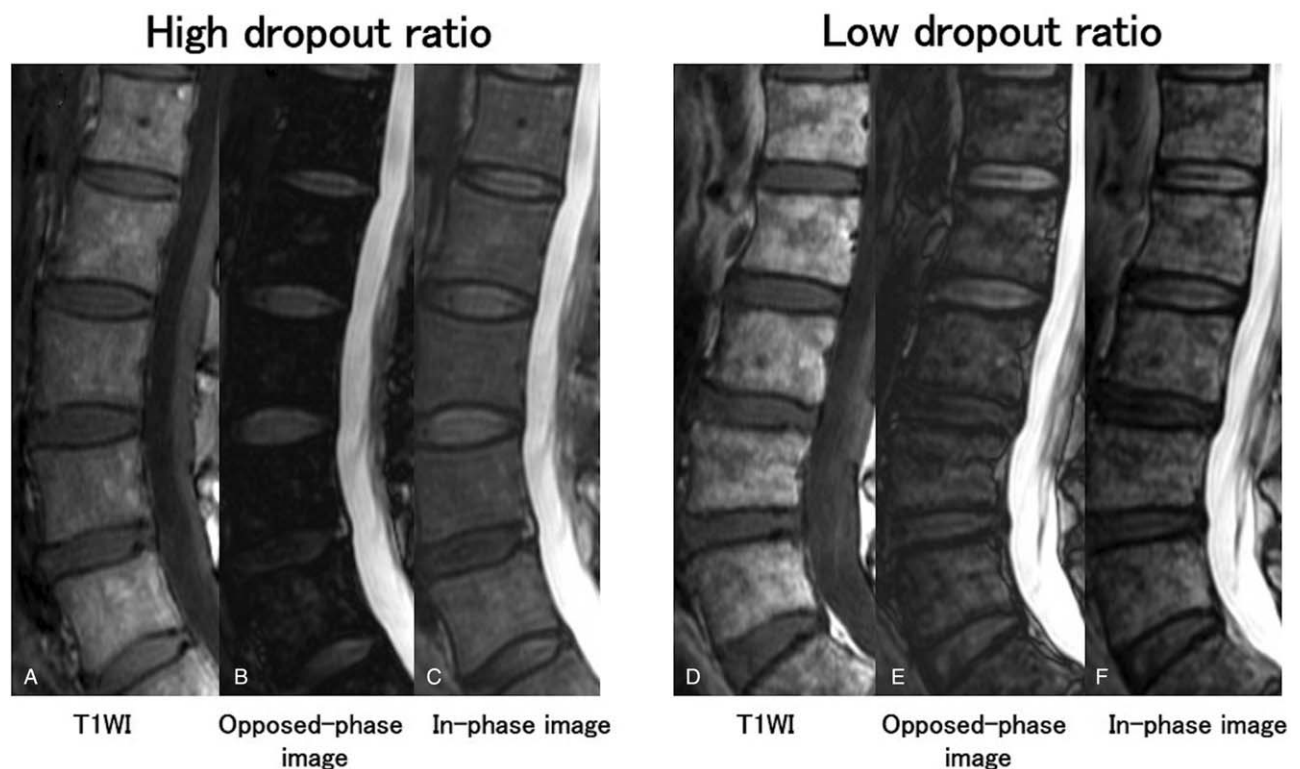


**Figure 6.** Sagittal MRI of a 55-year-old woman with symptomatic myeloma and high dropout ratio (DR) (left column: fat-signal fraction = 52.2%, DR = 85.8%, serum monoclonal protein level = 8470 mg/dL, hemoglobin level = 12.7 g/dL) and a 64-year-old woman with symptomatic myeloma and a low DR (right column: fat-signal fraction = 73.5%, DR = 44.9%, serum monoclonal protein level = 3930 mg/dL, hemoglobin level = 9.8 g/dL). (A) and (D), T1-weighted images; (B) and (E), opposed-phase images; (C) and (F), in-phase images. Despite differences in DR between the 2 patients, clinical stage, serum monoclonal protein level, and hemoglobin level were similar. DR = dropout ratio.



ADC value of  $0.597 \times 10^{-3} \text{ mm}^2/\text{s}$  for differentiating diffuse and normal patterns on conventional (mainly T1-weighted) MRI. ADC measurements can be affected by the choice of b-value as well as by technical factors, including the imaging parameters. There is currently no established b-value for the evaluation of BM characteristics, including for MM<sup>[22]</sup>. Newer diffusion methods such as the intravoxel incoherent motion-MRI, in comparison with the pathological findings, might play a role in quantifying marrow lesions.

Regarding fluorodeoxyglucose positron emission tomography, the IMWG minimal residual disease criteria have integrated fluorodeoxyglucose positron emission tomography for evaluation of BM with residual disease<sup>[19]</sup>. However, an optimal maximum standard uptake value threshold has not been determined for diffuse myelomatous lesions.

In the present study, the findings of an uneven proportion of fat and water protons in the BM had clinical significance for patients with MM. For the group classified as water-dominant by CSI, clinical indices such as serum M protein and BMPC% had significant negative correlations with DR. This result indicates that BM with low DR on CSI was indicative of advanced disease with high cellularity because these clinical indices are usually related to tumor burden. In addition, several reports have demonstrated that diffuse MRI abnormality (ie, not variegated or normal pattern) in the BM is related to the prognosis of MM.<sup>[1,4]</sup> Therefore, the water-dominant group with low DR on CSI could have a poorer prognosis than with high DR; however, this is beyond the scope of the current study. In contrast, for fatty marrow, no significant correlation was demonstrated between DR and clinical factors. We consider that tumor cells and significant hematopoietic BM might coexist in the BM of patients with mild to moderate myeloma, which resulted in tumor mass not being reflected on CSI, although there could also be hematopoietic marrow reconversion coexisting with myelomatous infiltration in advanced myeloma due to decreased hemoglobin level.

This study has several limitations. First, the number of patients was small, which restricted the statistical analyses performed and thus could have impaired the explanatory power for interpreting CSI for evaluating myelomatous cell infiltration into BM, and test-retest reproducibility could not be assessed. Second, as we used a conventional IDEAL sequence, we could not implement corrections for relaxation and noise bias. We did not use a small flip angle for the excitation RF pulses to approach proton-density weighting, which may have caused quantification errors. In addition, integration of corrections of  $T_2^*$  relaxation into the IDEAL sequence would have enabled more accurate FF measurement<sup>[23–26]</sup>. Third, several other factors could have caused signal alteration in the control group; for example, mild BM edema or degenerative disc disease, as several of the control subjects had lumbago or pain in the lower extremities. However, we assessed the L1-L3 vertebral bodies, which are not usually vulnerable to degenerative disc disease. For ethical reasons, we did not recruit healthy control subjects from the local community. Lastly, we did not include iliac bone in this study, even though marrow in the iliac bone had been sampled both pre- and post-treatment. As skeletal involvement by MM shows a heterogeneous distribution, we considered that we could evaluate the BM status more reliably using the mean value of signal intensity obtained from three vertebral bodies than from a small area in the posterior part of the iliac bone.

## 5. Conclusion

CSI proved ineffective for differentiating myelomatous infiltration from hematopoietic BM. This finding indicates that it might be difficult to differentiate between regrowth of hematopoietic BM and minimal residual disease, or relapse after chemotherapy. For MM patients with relatively high BM cellularity, a small signal drop on the OP images indicated a higher tumor burden. For BM with relatively low cellularity, disease severity was not reflected by CSI.

## Author contributions

**Conceptualization:** Miyuki Takasu, Takayuki Tamura.

**Data curation:** Miyuki Takasu, Keizo Tanitame, Yasutaka Baba, Takayuki Tamura, Shota Kondo, Shogo Maeda.

**Formal analysis:** Miyuki Takasu, Keizo Tanitame.

**Funding acquisition:** Miyuki Takasu.

**Investigation:** Miyuki Takasu, Keizo Tanitame, Yasutaka Baba, Yuji Akiyama, Takayuki Tamura, Shota Kondo, Shogo Maeda, Akira Sakai.

**Methodology:** Miyuki Takasu, Takayuki Tamura.

**Project administration:** Kazuo Awai.

**Resources:** Yuji Akiyama, Takayuki Tamura, Akira Sakai, Kazuo Awai.

**Software:** Yuji Akiyama, Takayuki Tamura.

**Supervision:** Takayuki Tamura.

**Validation:** Miyuki Takasu.

**Visualization:** Miyuki Takasu, Yuji Akiyama, Takayuki Tamura.

**Writing – original draft:** Miyuki Takasu.

**Writing – review & editing:** Miyuki Takasu.

## References

- [1] Mouloupoulos LA, Gika D, Anagnostopoulos A, et al. Prognostic significance of magnetic resonance imaging of bone marrow in previously untreated patients with multiple myeloma. *Ann Oncol* 2005;16: 1824–1328.
- [2] Lecouvet FE, Vande Berg BC, Michaux L, et al. Stage III multiple myeloma: clinical and prognostic value of spinal bone marrow MR imaging. *Radiology* 1998;209:653–60.
- [3] Mouloupoulos LA, Dimopoulos MA, Kastritis E, et al. Diffuse pattern of bone marrow involvement on magnetic resonance imaging is associated with high risk cytogenetics and poor outcome in newly diagnosed, symptomatic patients with multiple myeloma: a single center experience on 228 patients. *Am J Hematol* 2012;87:861–4.
- [4] Hillengass J, Fechtner K, Weber MA, et al. Prognostic significance of focal lesions in wholebody magnetic resonance imaging in patients with asymptomatic multiple myeloma. *J Clin Oncol* 2010;28:1606–10.
- [5] Dixon WT. Simple proton spectroscopic imaging. *Radiology* 1984;153: 189–94.
- [6] Zajick DC Jr, Morrison WB, Schweitzer ME, et al. Benign and malignant processes: normal values and differentiation with chemical shift MR imaging in vertebral marrow. *Radiology* 2005;237:590–6.
- [7] Costa FM, Canella C, Vieira FG, et al. The usefulness of chemical-shift magnetic resonance imaging for the evaluation of osteoid osteoma. *Radiol Bras* 2018;51:156–61.
- [8] Swartz PG1, Roberts CC. Radiological reasoning: bone marrow changes on MRI. *AJR Am J Roentgenol* 2009;193:S1–4.
- [9] Reeder SB, Pineda AR, Wen Z, et al. Iterative decomposition of water and fat with echo asymmetry and least-squares estimation (IDEAL): application with fast spin-echo imaging. *Magn Reson Med* 2005;54:636–44.
- [10] Guiu B, Petit JM, Loffroy R, et al. Quantification of liver fat content: comparison of triple-echo chemical shift gradient-echo imaging and in vivo proton MR spectroscopy. *Radiology* 2009;250:95–102.
- [11] Hines CD, Yu H, Shimakawa A, et al. Quantification of hepatic steatosis with 3-T MR imaging: validation in ob/ob mice. *Radiology* 2010;254: 119–28.
- [12] Takasu M, Tani C, Sakoda Y, et al. Iterative decomposition of water and fat with echo asymmetry and least-squares estimation (IDEAL) imaging



- of multiple myeloma: initial clinical efficiency results. *Eur Radiol* 2012;22:1114–21.
- [13] Takasu M, Tamura T, Kaichi Y, et al. Magnetic resonance evaluation of multiple myeloma at 3.0 Tesla: how do bone marrow plasma cell percentage and selection of protocols affect lesion conspicuity? *PLoS One* 2014;28:e85931.
- [14] Aoki T, Yamaguchi S, Kinoshita S, et al. Quantification of bone marrow fat content using iterative decomposition of water and fat with echo asymmetry and least-squares estimation (IDEAL): reproducibility, site variation and correlation with age and menopause. *Br J Radiol* 2016;89:20150538.
- [15] International Myeloma Working Group. Criteria for the classification of monoclonal gammopathies: multiple myeloma and related disorders: a report of the International Myeloma Working Group. *Br J Haematol* 2003;121:749–57.
- [16] Vogler JB 3rd, Murphy WA. Bone marrow imaging. *Radiology* 1988;168:679–93.
- [17] Palumbo A, Waage A, Hulin C, et al. Safety of thalidomide in newly diagnosed elderly myeloma patients: a meta-analysis of data from individual patients in six randomized trials. *Haematologica* 2013;98:87–94.
- [18] Bringhen S, Mateos MV, Zweegman S, et al. Age and organ damage correlate with poor survival in myeloma patients: meta-analysis of 1435 individual patient data from 4 randomized trials. *Haematologica* 2013;98:980–7.
- [19] Kumar S, Paiva B, Anderson KC, et al. International Myeloma Working Group consensus criteria for response and minimal residual disease assessment in multiple myeloma. *Lancet Oncol* 2016;17:e328–46.
- [20] Swartz PG, Roberts CC. Radiological reasoning: bone marrow changes on MRI. *AJR Am J Roentgenol* 2009;193:S1–4.
- [21] Koutoulidis V, Fontara S, Terpos E, et al. Quantitative Diffusion-weighted imaging of the bone marrow: an adjunct tool for the diagnosis of a diffuse MR imaging pattern in patients with multiple myeloma. *Radiology* 2017;282:484–93.
- [22] Koutoulidis V, Papanikolaou N, Moulopoulos LA. Functional and molecular MRI of the bone marrow in multiple myeloma. *Br J Radiol* 2018;91:20170389.
- [23] Yu H, McKenzie CA, Shimakawa A, et al. Multiecho reconstruction for simultaneous water-fat decomposition and T2\* estimation. *J Magn Reson Imaging* 2007;26:1153–61.
- [24] Yu H, Shimakawa A, McKenzie CA, et al. Multiecho water-fat separation and simultaneous R2\* estimation with multifrequency fat spectrum modeling. *Magn Reson Med* 2008;60:1122–34.
- [25] Colgan TJ, Van Pay AJ, Sharma SD, et al. Diurnal variation of proton density fat fraction in the liver using quantitative chemical shift encoded MRI. *J Magn Reson Imaging* 2020;51:407–14.
- [26] Procter AJ, Sun JY, Malcolm PN, et al. Measuring liver fat fraction with complex based chemical shift MRI: the effect of simplified sampling protocols on accuracy. *BMC Medical Imaging* 2019;19:14.